Images of the Fermi Surface in Phonon Spectra of Metals*

E. J. WOLL, JR.,† AND W. KOHN

Department of Physics, University of California, San Diego, La Jolla, California

(Received December 11, 1961)

This paper contains semiquantitative considerations concerning images of the Fermi surface in the phonon spectra of various metals. Anomalies in the phonon dispersion curves, as well as discontinuities of the phonon lifetime, are discussed.

1. INTRODUCTION

IT has been pointed out that, because of the response of conduction electrons to motion of the ions, images of the Fermi surface may be expected to appear in metallic phonon spectra.[1] In the space of phonon-wave vectors $\mathbf{q}$ there will be surfaces S on which the frequency varies abruptly with $\mathbf{q}$. The location of these surfaces is determined by the shape of the Fermi surface. For example, in the case of a simply connected convex Fermi surface, one has the relation

$$\mathbf{q}+\mathbf{K}=2\mathbf{k}, \tag{1.1}$$

where $\mathbf{q}$ is a phonon wave vector on S, $\mathbf{K}$ is a reciprocal lattice vector, and $\mathbf{k}$ is a wave vector on the Fermi surface. Similar effects may also be expected in spin-wave spectra.[1,2]

Recently, Brockhouse *et al.*[3] have discovered such images in the phonon spectrum of lead. This group has also reported that no image effects could be detected in the spectrum of sodium. It may be hoped that this effect will contribute to our knowledge of the shapes of metallic Fermi surfaces, particularly since the rule for constructing the Fermi surface, Eq. (1.1), is very simple.

The present paper attempts some semiquantitative estimates of the actual magnitude of image effects. In Sec. 2 the phonon spectrum, including image effects, is calculated using a model of ions immersed in and screened by a uniform electron gas. The magnitude of the calculated image effects (of the order of a few percent) is comparable to those observed in lead.[3]

Section 3 refines this model to take into account the Bloch character of the electron wave functions. Using assumptions which are believed to be valid for certain metals, including sodium and aluminum, it is found that this refinement reduces the image effects by a remarkably large factor, of order 10^{-2}. It may be remarked here that the magnitude of image effects is directly related to the magnitude of electron-phonon Umklapp processes.

In Sec. 4 a second but closely related image effect is discussed. A phonon can decay with the generation of an electron-hole pair. This decay rate has a discontinuity, as a function of $\mathbf{q}$, on the same surfaces S determined by (1.1). This discontinuity may be experimentally observable in the widths of phonon frequencies.

2. UNIFORM ELECTRON GAS MODEL

We wish to determine the vibration frequencies of an array of ions immersed in a uniform electron gas. The first step in this calculation is the determination of an effective potential energy of interaction between a pair of ions.

We first consider the electronic charge density built up when a single ion is placed in a uniform gas. Let the ion be situated at the coordinate origin, and denote the unscreened-ionic potential by $QV(\mathbf{r})$, where Q is the ionic charge. Then the Hartree Hamiltonian for an individual electron is

$$H=H_0+QeV(\mathbf{r})+e^2V_e(\mathbf{r}), \tag{2.1}$$

where H_0 is the kinetic energy of the electrons, and $e^2V_e(\mathbf{r})$ is the Hartree potential of interaction with the displaced electron charge.[4] This potential must satisfy Poisson's equation

$$\nabla^2 V_e(\mathbf{r})=-4\pi[N(\mathbf{r})-N_0], \tag{2.2}$$

where $N(\mathbf{r})$ and N_0 are, respectively, the perturbed and unperturbed electron densities.

We introduce the volume of the box, Ω, and Fourier transforms according to the notation

$$v(\mathbf{p})=\int_\Omega V(\mathbf{r})e^{-i\mathbf{p}\cdot\mathbf{r}}d^3r. \tag{2.3}$$

Then, by first-order perturbation theory, the electron wave functions can be written as

$$\psi_\mathbf{k}=\Omega^{-\frac{1}{2}}\left(e^{i\mathbf{k}\cdot\mathbf{r}}+\Omega^{-1}\sum_\mathbf{p}\frac{Qev(\mathbf{p})+e^2v_e(\mathbf{p})}{E_\mathbf{k}-E_\mathbf{k+p}}e^{i(\mathbf{k}+\mathbf{p})\cdot\mathbf{r}}\right), \tag{2.4}$$

where $E_\mathbf{k}$ are the unperturbed energies. From this expression $n(\mathbf{p})$ can be computed. Substitution into the

[1] W. Kohn, Phys. Rev. Letters **2**, 393 (1959).
[2] E. J. Woll and S. J. Nettel, Phys. Rev. **123**, 796 (1961).
[3] B. N. Brockhouse, K. R. Rao, and A. D. B. Woods, Phys. Rev. Letters **7**, 93 (1961).

[4] Because of the charge neutrality of the entire system, the zero-wave-number Fourier components of all potentials are consistently dropped.

Fourier transform of (2.2) gives

$$v_e(\mathbf{p}) = 4\pi Q e \frac{W(\mathbf{p})v(\mathbf{p})}{p^2 + 4\pi e^2 W(\mathbf{p})}, \qquad (2.5)$$

where

$$W(\mathbf{p}) = -4\Omega^{-1} \sum_{k<k_F}(E_k - E_{k+p})^{-1}, \qquad (2.6)$$

and the summation in (2.6) runs over the interior of the Fermi sphere of radius k_F. This expression for $v_e(\mathbf{p})$ can be substituted into (2.4), and the electronic charge density $n(\mathbf{p})$ computed. The result is

$$n(\mathbf{p}) = \frac{Qe p^2 v(\mathbf{p})W(\mathbf{p})}{p^2 + 4\pi e^2 W(\mathbf{p})}. \qquad (2.7)$$

The interaction energy between two ions can now be viewed as having two parts: a direct interaction between the two ions, and an interaction of the second ion with the electronic charge displaced by the first. The total energy of interaction when the second ion is at $\mathbf{r}$ is then

$$\Phi(\mathbf{r}) = \Omega^{-1} \sum_{\mathbf{p}} \varphi(\mathbf{p})e^{i\mathbf{p}\cdot\mathbf{r}}, \qquad (2.8)$$

where

$$\varphi(\mathbf{p}) = \left[\frac{Q^2 p^2 v^2(\mathbf{p})}{4\pi}\right]\left(1 - \frac{4\pi e^2 W(\mathbf{p})}{p^2 + 4\pi e^2 W(\mathbf{p})}\right). \qquad (2.9)$$

The first term describes direct interaction between the ions, and the second the reduction due to electronic screening. This is exactly the result found by Langer and Vosko.[5]

Calculation of the vibration frequencies of a Bravais lattice is now simple. We denote the equilibrium position of the mth ion by $\mathbf{R}_m$, and its excursion by $\mathbf{r}_m$. Then, to first order in the excursions, the force on the mth ion is

$$\mathbf{F}_m = -\nabla_m \sum_n \Phi_{mn}$$
$$= -\Omega^{-1} \sum_{\mathbf{p}} \sum_n \exp[i\mathbf{p}\cdot(\mathbf{R}_m - \mathbf{R}_n)]$$
$$\mathbf{p}\cdot(\mathbf{r}_m - \mathbf{r}_n)\mathbf{p}\varphi(\mathbf{p}), \qquad (2.10)$$

and the equations of motion are, of course,

$$\mathbf{F}_m = M\ddot{\mathbf{r}}_m, \qquad (2.11)$$

where M is the ionic mass. Equations (2.10) and (2.11) are solved by the Ansatz

$$\mathbf{r}_m = \boldsymbol{\varepsilon} \cos(\mathbf{q}\cdot\mathbf{R}_m - \omega t), \qquad (2.12)$$

where $\boldsymbol{\varepsilon}$ is the unit polarization vector, $\mathbf{q}$ the propagation
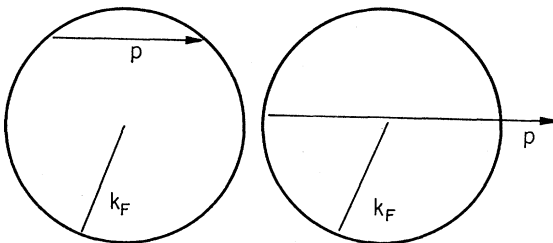

FIG. 1. Virtual excitations for the two cases $p<2k_F$ and $p>2k_F$.

[5] J. S. Langer and S. H. Vosko, J. Phys. Chem. Solids 12, 196 (1959).

vector, and

$$\omega^2 = (N_I/M)\{A(\mathbf{q}) + \sum_{K\neq0}[A(\mathbf{K}+\mathbf{q}) - A(\mathbf{K})]\}. \qquad (2.13)$$

Here N_I is the number of ions per unit volume, the sum runs over all reciprocal lattice vectors $\mathbf{K}$, and

$$A(\mathbf{p}) = (\mathbf{p}\cdot\boldsymbol{\varepsilon})^2\varphi(\mathbf{p})$$
$$= \left(\frac{Q^2}{4\pi}\right)(\mathbf{p}\cdot\boldsymbol{\varepsilon})^2 p^2 v^2(\mathbf{p})\left(1 - \frac{4\pi e^2 W(\mathbf{p})}{p^2 + 4\pi e^2 W(\mathbf{p})}\right). \qquad (2.14)$$

The Fermi surface images in the phonon spectrum arise from the nonanalytic behavior of $W(\mathbf{p})$ at $p=2k_F$. This is due to the fact that a perturbation of wave number $p<2k_F$ can produce virtual electron-hole pairs with excitation energies beginning at zero [see Eqs. (2.4), (2.6), and Fig. 1], while for $p>2k_F$ the minimum excitation energy is proportional to the finite value $(p-k_F)^2 - k_F^2 = p(p-2k_F)$. Thus, there is a rapid drop in the ability of the conduction electrons to screen an electrostatic field of wave number p, as p increases through the value $2k_F$.

This, together with Eq. (2.12), implies the following simple rule for the vibration frequencies: If, with increasing value of $\mathbf{q}$, the vector $\mathbf{q}+\mathbf{K}$ (for some $\mathbf{K}$) passes through the Fermi surface from the inside to the outside, the frequency ω rises abruptly; if from outside to the inside, the frequency drops. The reported observations[3] conform with this rule.

The analytic form of $W(\mathbf{p})$ is

$$W(\mathbf{p}) = \left(\frac{mk_F}{2\pi^2\hbar^2}\right)\left[1 + \frac{1}{pk_F}\left(\frac{k_F^2 - p^2}{4}\right)\ln\left|\frac{p+2k_F}{p-2k_F}\right|\right]. \qquad (2.15)$$

This shows that the above-mentioned "abrupt" changes are logarithmic infinities in the slope.

The frequency spectrum (2.13) has been computed for constants corresponding to aluminum[6] for propagation vectors in directions of high symmetry. Dispersion curves for $\mathbf{q}$ in the [111] direction, for both directions of polarization, are plotted in Fig. 2. While the model of this section almost certainly overestimates the prominence of image effects in aluminum (see Sec. 3), the qualitative similarity of Fig. 2 to the observed phonon spectrum in lead (shown in Fig. 3) is quite striking.

3. BLOCH ELECTRONS IN THE BARDEEN APPROXIMATION

In a classic paper on electrical conductivity of metals, Bardeen[7] succeeded in treating the interaction of lattice vibrations with Bloch electrons by making certain simplifying assumptions about the electron wave functions. In this section we shall estimate the magnitude of image effects under the same assumptions.

We first calculate the change in electronic charge

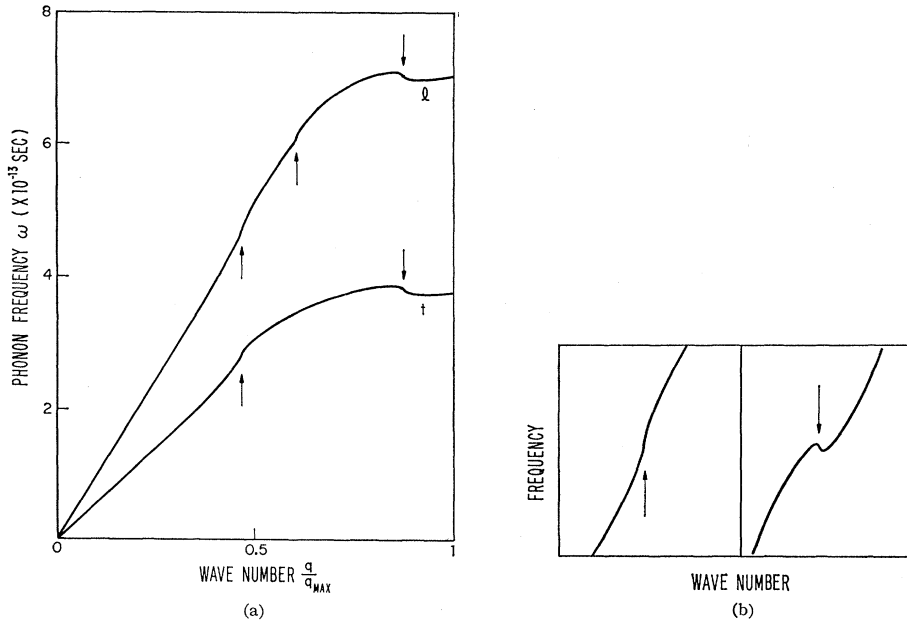[7] J. Bardeen, Phys. Rev. 52, 688 (1937).

(a)

(b)

FIG. 2. (a) Dispersion curves calculated from the uniform electron gas model for constants corresponding to aluminum. These curves are for the [111] direction of reciprocal space; "l" and "t" label the longitudinal and transverse polarization branches. Fermi images are indicated by arrows. While the considerations of Sec. 3 suggest that the model used is inappropriate for aluminum, kinks of this general order may well appear in other metals. (b) Characteristic "upward" and "downward" anomalies of the dispersion curves. Scales are enlarged 5× from the scales of Fig. 2(a). While no simple downward anomaly occurs in the case of aluminum, the example shown here should be helpful in interpretation of such anomalies where they do appear, as in the case of lead.

density set up when one ion is displaced. We take as electron Hamiltonian

$$H = H_0 + Qe\mathbf{r}_1 \cdot \nabla V(\mathbf{r}) + e^2 V_e(\mathbf{r}), \qquad (3.1)$$

where H_0 contains the electron-kinetic energy, the energy of interaction with the ions in their equilibrium positions, and the Hartree interaction with the other Bloch electrons; $\mathbf{r}_1$ is the displacement of ion 1 from its equilibrium position at the origin; $QeV(\mathbf{r})$ is the ionic potential, and $e^2V_e(\mathbf{r})$ is the self-consistent electron potential due to displacement of the ion.

We first assume, following Bardeen,[7] that the matrix element $(\mathbf{k}+\mathbf{p}|\nabla V(\mathbf{r})|\mathbf{k})$, taken between Bloch states, has negligible $\mathbf{k}$ dependence. [This is certainly so if the Bloch functions can be written in the form $u_0(\mathbf{r}) \times \exp(i\mathbf{k} \cdot \mathbf{r})$.] We then define $v^*(\mathbf{p})$ according to the equation

$$\mathbf{p}v^*(\mathbf{p}) \equiv -i\Omega(\mathbf{k}+\mathbf{p}|\nabla V(\mathbf{r})|\mathbf{k}). \qquad (3.2)$$

At this point, instead of making a fully self-consistent calculation with the Bloch wave functions, we recognize that the important effect of the term $e^2V_e(\mathbf{r})$ is the screening of the ionic potential, and we follow Bardeen in saying that screening by Bloch electrons will be roughly the same as free-electron screening. Then, instead of keeping the term $e^2V_e(\mathbf{r})$ in (3.1), we simply reduce $v^*(\mathbf{p})$ by the factor $p^2/[p^2 + 4\pi e^2 W^*(\mathbf{p})]$, where

$$W^*(\mathbf{p}) = (m^*/m)W(\mathbf{p}), \qquad (3.3)$$

with m^* the effective electronic mass. Since the effect

of screening is large only for small $\mathbf{p}$ while our region of interest is $p \sim 2k_F$, we do not expect this approximation to affect our results significantly.

With these assumptions the electron wave functions, perturbed by the displacement of ion 1, become

$$\psi_\mathbf{k} = \varphi_\mathbf{k} + 4\pi Qe\Omega^{-1} \sum_\mathbf{p} (E_\mathbf{k} - E_{\mathbf{k}+\mathbf{p}})^{-1}$$
$$\times (\mathbf{r}_1 \cdot i\mathbf{p})v^*(\mathbf{p})p^2[p^2 + 4\pi e^2 W^*(\mathbf{p})]^{-1}\varphi_{\mathbf{k}+\mathbf{p}}, \qquad (3.4)$$

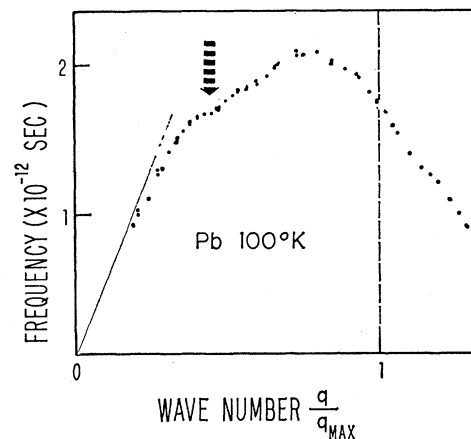where $\varphi_\mathbf{k}$ are the Bloch functions and $E_\mathbf{k}$ are the eigenvalues of H_0.

FIG. 3. Measured dispersion curve for longitudinal polarization, for the [110] direction in lead. (Reproduced from Brockhouse et al.; see reference 3.) The position of a large downward anomaly is roughly indicated by the arrow. The qualitative similarity of these results to the theoretical curve of Fig. 2 is quite striking.

A second displaced ion interacts electrostatically with the first ion and the displaced electron charge. The energy of interaction with the second ion at R_2+r_2 is

$$\Phi_{12}=\frac{Q^2}{4\pi\Omega}\sum_p \exp[i\mathbf{p}\cdot(\mathbf{R_1}-\mathbf{R_2})]$$

$$\times\left\{\exp[i\mathbf{p}\cdot(\mathbf{r_1}-\mathbf{r_2})]p^2v^2(\mathbf{p})\right.$$

$$\left.-(\mathbf{p}\cdot\mathbf{r_1})(\mathbf{p}\cdot\mathbf{r_2})\frac{4\pi e^2W^*(\mathbf{p})p^2v^{*2}(\mathbf{p})}{p^2+4\pi e^2W^*(\mathbf{p})}\right\}, \quad (3.5)$$

where again the first term describes direct interaction between the ions and the second term the reduction due to electron screening.

The calculation of vibration frequencies proceeds essentially as in Sec. 2, and we find

$$\omega^2=(N_I/M)\{A(\mathbf{q})+\sum_{K\neq0}[A(\mathbf{K+q})-A(\mathbf{K})]\}, \quad (3.6)$$

where

$$A(\mathbf{p})=\frac{Q^2}{4\pi}(\mathbf{p}\cdot\boldsymbol{\varepsilon})^2$$

$$\times\left[p^2v^2(\mathbf{p})-\frac{4\pi e^2W^*(\mathbf{p})p^2v^{*2}(\mathbf{p})}{p^2+4\pi e^2W^*(\mathbf{p})}(1-\delta_{p,K})\right]. \quad (3.7)$$

Except for the appearance of effective masses and the substitution of the factor $v^{*2}(\mathbf{p})(1-\delta_{p,K})$ for $v^2(\mathbf{p})$, this result is identical to (2.14). The size of image effects is determined by the magnitude of $v^*(\mathbf{p})$ for $p=2k_F$. For sodium, Bardeen gives

$$Qev^*(\mathbf{p})=(C+4\pi Qe/p^2)G(pr_s), \quad (3.8)$$

where r_s is the radius of the unit cell approximated as a sphere, and

$$G(x)=3x^{-3}(\sin x-x\cos x), \quad [G(0)=1]. \quad (3.9)$$

The constant C is related to the curvature of the Bloch functions near the edge of the unit cell, and is small (less than 10% of $4\pi e^2/p^2$ in sodium for $p=2k_F$).[8] Here we ignore C and note that the important modification of the result of the last section is a reduction of electron-shielding terms by the factor $G^2(pr_s)$. Now $G^2(x)$ is a rapidly decreasing function of x. In fact, for all metals $G(|\mathbf{K+q}|r_s)$ with $\mathbf{q}$ in the first Brillouin zone and $\mathbf{K}\neq0$ is small compared to unity, in general of order 0.1. As a result, the electronic contribution to $A(\mathbf{p})$ [the second term in (3.7)] can be to a good approximation neglected in the sum over $\mathbf{K}$ occurring in (3.6). In particular, the magnitude of the image effects is reduced by a factor of order 10^{-2}.

These considerations are in the same spirit as the discussion of the elastic constants of sodium by Bardeen and Pines,[8] who obtain agreement with experiment to within 10%. Their results can be obtained from (3.6) and (3.7) if the second term in (3.7) is dropped for $\mathbf{p}\neq\mathbf{q}$.

[8] J. Bardeen and D. Pines, Phys. Rev. **99**, 1140 (1955).

We expect our estimate of Bloch wave effects to be somewhat drastic. It seems to be accurate for sodium and for certain other metals (including aluminum) whose characteristics are more fully discussed in the Appendix. It should be noted, in this connection, that image effects are small in these cases for the reason that Umklapp processes do not make an important contribution to the electron-ion interaction. This should not be true in general. If, for some metals, Umklapp processes do make an important contribution to the electron-ion interaction, we should expect this fact to be reflected in some characteristics of the metal. Thus, clues may appear from an examination of metallic characteristics as to whether Fermi images are observable. Two such clues suggest themselves. First, resistivity of metals with Umklapp processes should be somewhat higher than is to be expected from simple scaling. Second, since only Umklapp processes screen the transverse lattice vibrations, metals without Umklapps will have transverse frequencies (for small $\mathbf{q}$) entirely determined by direct ionic interaction. We have, of course, neglected ion-overlap contributions to the frequency, so that transverse frequencies may be higher, by some unknown amount, than our formulas would predict. But at least the existence of unusually low transverse frequencies would imply that Umklapp processes were contributing.[9] In both of these effects lead shows the properties of a metal with Umklapp processes: the resistance is unusually high and the transverse frequencies, as judged by the Debye temperature, are unusually low. On the other hand, aluminum and sodium have resistance and Debye temperature in line with the general run of metals.

In summary, the nonobservation of image effects in sodium and aluminum is consistent with other empirical
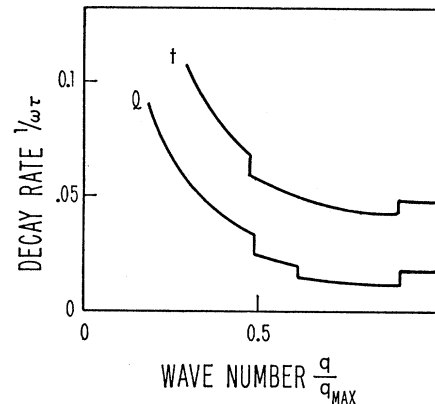

FIG. 4. Calculated phonon decay rate, expressed as a fraction of frequency, for $\mathbf{q}$ in the [111] direction of reciprocal space; "l" and "t" label the longitudinal and transverse polarization branches. The free-electron model has been used, with constants corresponding to aluminum. Decay rates for very small $\mathbf{q}$ are controlled by more complicated processes,[10] and are not given correctly by these curves. Again, the model used is probably inappropriate for aluminum, but breaks of such magnitude are expected to appear in other cases.

[9] We are indebted to Dr. Vosko for this remark. A more detailed discussion of this aspect by Dr. Vosko is in preparation.

properties of these metals and can also be concluded from *a priori* calculations. On the other hand, the observation of such effects in lead, while consistent with other empirical information, has not yet been explained on the basis of a detailed calculation.

4. PHONON LIFETIME

The lifetime of a phonon exposed to the hazard of decay into an electron-hole pair can be found by calculating the rate of energy absorption by the electron gas when the lattice is driven in one of its normal modes. We assume the electrons see screened ions, so the matrix element is taken to be reduced, as in Sec. 3, by the factor $p^2/[p^2+4\pi e^2W^*(\mathbf{p})]$. From first-order perturbation theory we find for the probability per unit time that the state $|\mathbf{k}+\mathbf{p})$ be excited from the state $|\mathbf{k})$, by interaction with the array of ions vibrating as in (2.12),

$$W_{\mathbf{k}+\mathbf{p},\mathbf{k}} = (\pi N_I^2 Q^2 e^2/2\hbar)$$
$$\times (\mathbf{p}\cdot\mathbf{\epsilon})^2 v^{*2}(\mathbf{p}) p^4 [p^2+4\pi e^2 W^*(\mathbf{p})]^{-2} \delta_{\mathbf{p},\mathbf{K}+\mathbf{q}}$$
$$\times [\delta(E_{\mathbf{k}+\mathbf{p}}-E_{\mathbf{k}}-\hbar\omega)$$
$$+\delta(E_{\mathbf{k}+\mathbf{p}}-E_{\mathbf{k}}+\hbar\omega)]. \quad (4.1)$$

The total energy absorbed by the electron gas per unit time is

$$E' = \sum_{\mathbf{k}}\sum_{\mathbf{p}} W_{\mathbf{k}+\mathbf{p},\mathbf{k}}(E_{\mathbf{k}+\mathbf{p}}-E_{\mathbf{k}}), \quad (4.2)$$

where $\sum_{\mathbf{k}}$ runs over all the states below the Fermi surface, and $\sum_{\mathbf{p}}$ runs over all electron states. $W_{\mathbf{k}+\mathbf{p},\mathbf{k}}$ is, except for the energy δ functions, independent of $\mathbf{k}$. Converting $\sum_{\mathbf{k}}$ into an integration and doing the integration over the δ functions gives a factor

$$\begin{array}{ll} m^{*2}\omega^2/2\pi^2\hbar^2 p & \text{for} \quad p<2k_F, \\ 0 & \text{for} \quad p>2k_F. \end{array} \quad (4.3)$$

The total energy absorption per unit time, expressed as a fraction of the total vibrational energy of the lattice, can be identified as the phonon-decay rate, or inverse lifetime:

$$1/\tau = (Q^2 e^2 N_I m^{*2}/\pi\hbar^3 M)\sum_{\mathbf{K}} B(\mathbf{K}+\mathbf{q}), \quad (4.4)$$

where

$$B(\mathbf{p}) = (\mathbf{p}\cdot\mathbf{\epsilon})^2 p^3 v^{*2}(\mathbf{p})[p^2+4\pi e^2 W^*(\mathbf{p})]^{-2}$$
$$\text{for} \quad p<2k_F, \quad (4.5)$$
$$=0 \quad\quad\quad\quad\quad \text{for} \quad p>2k_F.$$

The decay rates computed from (4.4) and (4.5)[10] display step-discontinuities on surfaces in $\mathbf{q}$ space where the condition $|\mathbf{q}+\mathbf{K}|=2k_F$ can be satisfied with any reciprocal lattice vector $\mathbf{K}$. These decay rates have been computed, taking for $v^*(\mathbf{p})$ the free-electron matrix element, for constants corresponding to aluminum. Curves for both directions of polarization for $\mathbf{q}$ in the [111] direction of reciprocal space are plotted in Fig. 4.

---

[10] Neglecting Umklapp processes as in Sec. 3, this result agrees with Pippard's result for attenuation of ultrasonic waves, in the limit where $\mathbf{q}$ is small but not so small as the reciprocal-electron mean free path from impurity scattering [A. B. Pippard, Phil. Mag. **46**, 1104 (1955)].

Again we note that, if $v^*(\mathbf{p})$ falls off faster than the free-electron approximation predicts, the magnitude of these discontinuities will be correspondingly reduced. In particular, for the case of sodium and aluminum, only the $\mathbf{K}=0$ term should appreciably contribute in (4.5), and no significant breaks should appear.

APPENDIX

Bardeen's calculation of the matrix element $(\mathbf{k}+\mathbf{p}|\nabla V(\mathbf{r})|\mathbf{k})$ uses the basic assumption that the electron wave functions, written in the Bloch form $u_{\mathbf{k}}(\mathbf{r})\exp(i\mathbf{k}\cdot\mathbf{r})$, can be approximated as $u_0(\mathbf{r})\exp(i\mathbf{k}\cdot\mathbf{r})$, where $u_0(\mathbf{r})$ is the lowest eigenfunction of the conduction-electron Hamiltonian. This assumption is, presumably, valid for monovalent metals; we shall attempt to show here that it can be replaced by two other assumptions: that the electron wave functions can be adequately represented by single orthogonalized plane waves (OPW),[11] and that each ion core is well confined within its unit cell.

This replacement of Bardeen's assumption is possible because the assumption has been used only to determine the properties of $u_{\mathbf{k}}(\mathbf{r})$ at the edge of the unit cell. The important properties are: first, that $u_{\mathbf{k}}(\mathbf{r})$ should have spherical symmetry in this region; second, that $\partial^2 u_{\mathbf{k}}(\mathbf{r})/\partial r^2$ evaluated at the cell wall should vary slowly with $\mathbf{k}$ and thus be replaceable by $\partial^2 u_0(\mathbf{r})/\partial r^2$; and third, that the value $u_{\mathbf{k}}(r_s)$ should not vary with $\mathbf{k}$. The OPW are constructed by adding to plane waves linear combinations of ion-core wave functions (with coefficients so chosen as to make the OPW orthogonal to all core states). For ions which are well confined within their own unit cells, then, the OPW necessarily have almost pure-plane wave character near the cell walls. Then $u_{\mathbf{k}}(\mathbf{r})$ will have spherical symmetry in this region, and will be in fact very nearly flat. The second derivative $\partial^2 u_{\mathbf{k}}/\partial r^2$ falls off with distance from the center of the cell in the same way as the ionic wave functions, and so will be very small near the cell wall. We may be tempted to neglect it entirely, but a better approximation will be to replace it by $\partial^2 u_0/\partial r^2$. The value $u_{\mathbf{k}}(r_s)$ will depend on $\mathbf{k}$ only through a normalization constant. If the largest ion-core wave function falls off as $\exp(-r/a)$, then the natural parameter for a power series expansion of the normalization constant is $(ka)^2$. From Froese's[12] calculations for the trivalent aluminum ion, for instance, we find $ka\sim k/5k_F$, so the variation of $u_{\mathbf{k}}(r_s)$ with $\mathbf{k}$ will be small, for k in the region of interest.

Bardeen's calculation of the electron-ion matrix element is thus seen to go through under our assumptions. The question of whether the single-OPW approximation is good in any particular metal is rather difficult to answer, unless a band calculation has shown rapid convergence for an expansion of the actual wave functions in series of OPW. This is exactly the case in aluminum, as can be seen from the work of Heine.[11]

---

[11] V. Heine, Proc. Roy. Soc. (London) **A240**, 340 (1957).
[12] C. Froese, Proc. Cambridge Phil. Soc. **53**, 206 (1957).